

# Terahertz wave emission from a liquid water film under the excitation of asymmetric optical fields

Qi Jin, Jianming Dai, Yiwen E, and Xi-Cheng Zhang

Citation: *Appl. Phys. Lett.* **113**, 261101 (2018); doi: 10.1063/1.5064644

View online: <https://doi.org/10.1063/1.5064644>

View Table of Contents: <http://aip.scitation.org/toc/apl/113/26>

Published by the [American Institute of Physics](#)

---

## Articles you may be interested in

[Detection of nonmagnetic metal thin film using magnetic force microscopy](#)

*Applied Physics Letters* **113**, 261601 (2018); 10.1063/1.5079763

[Distinguishing charge and strain coupling in ultrathin \(001\)-La<sub>0.7</sub>Sr<sub>0.3</sub>MnO<sub>3</sub>/PMN-PT heterostructures](#)

*Applied Physics Letters* **113**, 262901 (2018); 10.1063/1.5051324

[Generating bright gamma-ray pulses via ultra-intense laser colliding with a flying plasma layer](#)

*Applied Physics Letters* **113**, 264101 (2018); 10.1063/1.5064699

[Numerical prediction of the driving performance of liquid crystal actuators](#)

*Applied Physics Letters* **113**, 261901 (2018); 10.1063/1.5047560

[Biocompatible and degradable gelatin dielectric based low-operating voltage organic transistors for ultra-high sensitivity NH<sub>3</sub> detection](#)

*Applied Physics Letters* **113**, 263301 (2018); 10.1063/1.5054026

[Self-propelling Leidenfrost droplets on a variable topography surface](#)

*Applied Physics Letters* **113**, 243704 (2018); 10.1063/1.5056249

---



**Measure Ready**  
**M91 FastHall™ Controller**

A revolutionary new instrument  
for complete Hall analysis

**Lake Shore**  
CRYOTRONICS

# Terahertz wave emission from a liquid water film under the excitation of asymmetric optical fields

Qi Jin,<sup>1</sup> Jianming Dai,<sup>2</sup> Yiwen E,<sup>1</sup> and Xi-Cheng Zhang<sup>1,3,a)</sup>

<sup>1</sup>The Institute of Optics, University of Rochester, Rochester, New York 14627, USA

<sup>2</sup>Center for Terahertz Waves and School of Precision Instrument and Opto-electronics Engineering, Tianjin University, Tianjin 300072, China

<sup>3</sup>Beijing Advanced Innovation Center for Imaging Technology, Capital Normal University, Beijing 100037, China

(Received 6 October 2018; accepted 12 November 2018; published online 26 December 2018)

Liquid water excited by intense two-color laser pulses radiates electromagnetic waves at terahertz frequencies. Compared with one-color excitation, two-orders of magnitude enhanced terahertz energy are observed by using asymmetric optical excitation with the same total excitation pulse energy and focusing geometry. Modulation of the terahertz field is achieved via the coherent control approach. We find that modulated and unmodulated terahertz energies have, respectively, quadratic and linear dependence on the laser pulse energy. This work, as part of terahertz aqueous photonics, paves an alternative way of studying laser-liquid interactions and developing intense terahertz sources. *Published by AIP Publishing.* <https://doi.org/10.1063/1.5064644>

Terahertz (THz) wave generation through the tunnel ionization process in gases induced by two-color (fundamental frequency  $\omega$  and its second-harmonic  $2\omega$ ) femtosecond laser pulses<sup>1</sup> is a significant milestone in the THz community due to its impressive intensity, remarkably broad bandwidth, and applications in nonlinear interactions and THz spectroscopy.<sup>2–5</sup> The THz wave generation process and coherent control in the two-color case have been explained by a four-wave mixing model,<sup>1,6</sup> a transient photocurrent model,<sup>7–9</sup> or a full quantum model.<sup>10</sup> The transient photocurrent model will be used in this paper for the following discussions. In this model, a net photocurrent produced by asymmetric optical fields through the photoionization radiates THz waves. Compared with THz wave generation from gas plasmas induced by one-color ( $\omega$ ) laser pulses, the asymmetric electron motion introduced by the two-color laser fields leads to a net dipole moment and hence much stronger THz emission. By changing the relative phase  $\varphi$  between  $\omega$  and  $2\omega$  pulses, modulation of THz electric fields generated from air plasmas has been achieved.<sup>6,11–13</sup> The dependence of THz yield upon the relative phase  $\varphi$  in the case of gas plasma has already been investigated in Refs. 7–13.

Recently, liquids have been demonstrated as sources for THz waves by focusing sub-picosecond one-color (800 nm) laser pulses into a thin water film<sup>14</sup> or femtosecond laser pulses into a cuvette filled with target liquids.<sup>15</sup> The THz wave generation from liquids offers an opportunity for detailed investigations into laser-liquid interactions and THz spectroscopy. These works also indicate that the laser-induced breakdown and plasma behaviors in liquid materials play a critical role in the THz wave generation process. Thus, stronger THz emission and its modulation are expected by using the asymmetric excitation scheme in liquid water. Manipulation of strong THz emission would have widespread

applications in different research fields, such as THz nonlinear optics<sup>16,17</sup> and electron acceleration.<sup>18,19</sup>

In this work, THz wave generation from a thin water film under two-color laser excitation is investigated. The schematic diagram of the experimental setup is shown in Fig. 1. A femtosecond amplified laser with a central wavelength of 800 nm and a repetition rate of 1 kHz is used. Unless otherwise stated, the laser pulse duration used in the experiment is 50 fs. A type-I Beta Barium Borate ( $\beta$ -BBO) crystal is used for the generation of  $2\omega$  pulses through frequency-doubling, and an in-line phase compensator (PC) is applied to accurately control the relative phase between  $\omega$  and  $2\omega$  pulses by changing the mechanical insertion of one of the fused silica wedges.<sup>11</sup> The energy of  $2\omega$  pulses is about 10% of the entire excitation laser energy. Both  $\omega$  and  $2\omega$  pulses are vertically polarized after they pass through the PC. Subsequently,  $\omega$  and  $2\omega$  laser pulses are co-focused into

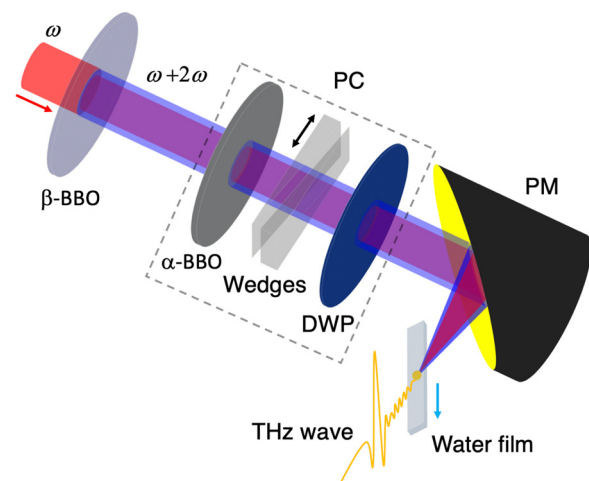


FIG. 1. Schematic diagram of the experimental setup. A phase compensator (PC) is applied to control the relative phase between  $\omega$  and  $2\omega$  pulses. DWP, dual-wavelength wave plate. PM, parabolic mirror with an effective focal length of 1-in.

<sup>a)</sup>Author to whom correspondence should be addressed: xi-cheng.zhang@rochester.edu

a 120- $\mu\text{m}$  thick water film by a 1-in. effective focal length parabolic mirror to generate THz waves. The focal point of the laser beam is set to be close to the center of the water film. A liquid jet is employed to obtain the water film. A high-resistivity silicon wafer is used as the filter to block the residual laser beams while allowing the THz waves to pass through. The THz electric field is detected by a 3-mm thick,  $\langle 110 \rangle$ -cut ZnTe crystal through electro-optical sampling (EOS).<sup>20</sup> Also, the corresponding THz energy is measured by a commercially available Golay cell with a combination of different filters that eventually blocked all the high-frequency components. The angle of incidence on the water film is optimized to be 61°.

Remarkably, the THz electric field generated from the two-color excitation scheme is about 10-times stronger than that from the one-color excitation scheme at the laser pulse duration of 50 fs, as shown in Fig. 2(a). The one-order of magnitude increased THz field indicates that two-orders of magnitude enhanced THz energy are achieved. The corresponding spectra are shown in Fig. 2(b). It is noteworthy that the enhancement of the THz electric field with the asymmetric excitation scheme in water may not be as high as that in air. This could arise from the fact that a short laser pulse duration works well for the case in air, but a longer pulse duration is favored in the ionization process in liquid water, where cascade ionization dominates.<sup>14,21,22</sup>

Comparatively, experimental results in the case of a longer laser pulse duration (300 fs), which is obtained by chirping the original 50 fs pulse, are shown in Figs. 2(c) and 2(d). The scales of the vertical axis in Figs. 2(a) and 2(c) are the same. Compared to the one-color case, the two-color excitation scheme provides 11% enhanced THz electric field when the pulse duration is 300 fs. Such a reduced enhancement rate may be caused by multiple effects. For example, the  $\omega$  and  $2\omega$  pulses may have uneven chirps, which reduces the

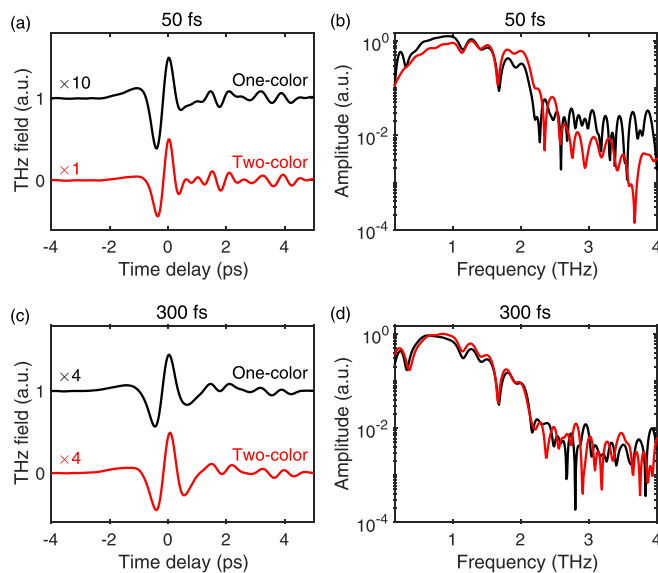


FIG. 2. Comparison of THz waves generated from a 120- $\mu\text{m}$  thick water film with one-color and two-color excitation schemes. (a) and (b) Comparison in the case of a short optical pulse duration (50 fs) in the time domain and frequency domain, respectively. (c) and (d) Comparison in the case of a long optical pulse duration (300 fs) in the time domain and frequency domain, respectively. Unified normalization ratios are labeled.

asymmetry of the ionized electron motion and finally decreases the overall generation efficiency of THz waves. The lower enhancement with a longer pulse duration can also result from the significant drop in second-harmonic generation efficiency as the pulse duration increases. In the experiment, the energy of  $2\omega$  pulse decreases by more than 60% when the pulse duration increases from 50 fs to 300 fs.

The enhancement of THz wave radiation with an asymmetric excitation scheme has previously been observed when air plasmas act as the THz source.<sup>6</sup> The electrons ionized from water molecules are regarded as quasi-free electrons,<sup>22</sup> and therefore the THz wave generation process in water resembles this process in air. Phenomenologically, the transient photocurrent model can be used to explain the generation process in water and would predict the modulation of THz fields generated from a water film as well, which is experimentally confirmed, as shown in Fig. 3. Specifically, Fig. 3(a) shows that the polarity of the THz electric field is completely flipped over by changing the relative phase  $\varphi$  by  $\pi$ . The THz waveforms are measured by EOS. The inset of Fig. 3(a) plots the THz field as a function of optical phase delay between  $\omega$  and  $2\omega$  pulses, which indicates that the

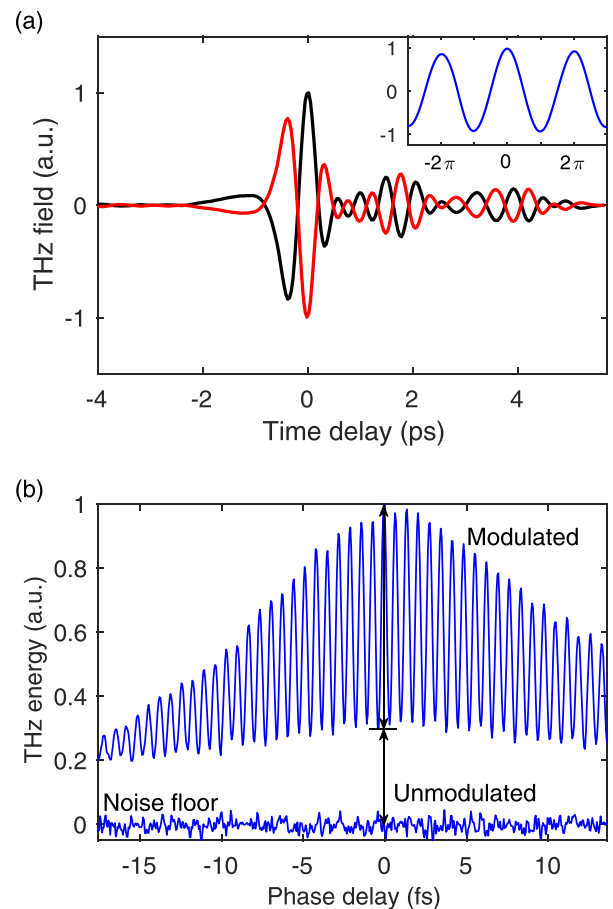


FIG. 3. Modulation of THz wave generation from a water film. (a) Comparison of THz waveforms obtained when the relative phase between  $\omega$  and  $2\omega$  pulses is changed by  $\pi$  through the change of the insertion of one of the wedges in the phase compensator. Inset: THz electric field as a function of the phase delay between  $\omega$  and  $2\omega$  pulses. (b) An overall phase scan for THz wave radiation from the water film obtained by gradually changing the phase between  $\omega$  and  $2\omega$  pulses while monitoring the THz energy by using a Golay cell. The range of the phase delay is limited by the full length of the wedge.

polarity of the THz electric field is gradually changed with the optical phase delay. Moreover, an overall phase scan for THz wave emission from the water film is obtained by gradually adjusting the phase between  $\omega$  and  $2\omega$  pulses at an attosecond-level accuracy while monitoring the THz energy with a Golay cell, as shown in Fig. 3(b). The noise floor is also shown in the figure. The modulated portion shows the phase modulation while the unmodulated portion remains blank at the bottom of the figure. By comparing the energy levels in the figure, the modulated and unmodulated components are estimated to be 70% and 30%, respectively. It is notable that similar modulation can be achieved with a longer optical pulse duration (300 fs) as well.

The modulated and unmodulated THz waves relate to different generation processes in the plasma. For further study, we measured the corresponding THz energy as a function of the excitation laser pulse energy. Figure 4 plots the THz energy as a function of the total excitation pulse ( $\omega$  and  $2\omega$ ) energy. The unmodulated THz energy (red circles) shows a linear dependence on the laser pulse energy. For the modulated THz energy (blue dots), the modulation does not appear until the excitation pulse energy is beyond 200  $\mu\text{J}$ . Subsequently, the measurement matches a quadratic fitting above the threshold. In addition, the energy dependence measured from EOS (blue squares) is coincident with the modulated result from the Golay cell.

Similar to the case in air, the modulated THz energy mainly comes from electron acceleration<sup>7-9</sup> in the transient photocurrent model, while in the full quantum model, the modulated THz radiation may also result from the buildup of bremsstrahlung from electron-atom collisions.<sup>10</sup> In contrast, the unmodulated THz energy may arise from multiple physical processes. For instance, a spatial net charge distribution created by the ponderomotive force radiates THz waves.<sup>23</sup> Since no threshold is observed for the unmodulated portion, the THz wave emission can be attributed to part of the broadband radiation from the combination of thermal bremsstrahlung

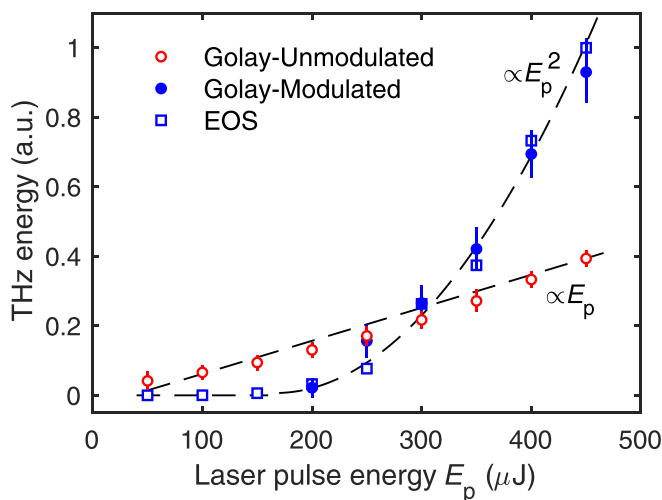


FIG. 4. Normalized THz energy from liquid water as a function of the total excitation laser pulse ( $\omega$  and  $2\omega$ ) energy. Blue squares, THz energy calculated from the temporal integral of the THz waveform measured by EOS. Blue dots, modulated THz energy measured by the Golay cell. Red circles, unmodulated THz energy measured by the Golay cell. The maximum pulse energy is limited by the available laser pulse energy in the experiment.

from electrons and electron-ion recombination.<sup>24</sup> Moreover, the energy dependence in Fig. 4 indicates that the ratio of the modulated THz energy to unmodulated THz energy increases with the laser pulse energy. The unmodulated component is stronger with weak excitation pulses while the modulated component will dominate if intense laser pulses are used.

In consideration of the fact that the liquid source can quickly replenish itself due to its fluidity, the THz wave emission can be dramatically scaled up by increasing the excitation laser energy, which reveals liquid water's potentiality to emit intense THz waves. Although no saturation occurs in Fig. 4 when the laser pulse energy is up to 450  $\mu\text{J}$ , it is worth mentioning that the saturation should be observed when the excitation energy is sufficiently high. The measured THz electric field strength is estimated as 1.1 kV/cm when the excitation laser pulse energy is 450  $\mu\text{J}$ . Realistically, the measured value is much weaker than the generated THz radiation due to the absorption of the water film itself and total internal reflection on the water-air boundary, etc.

When the optical beam is focused into the water film, it will also possibly create air plasmas located close to the air-water interface and water-air interface. Thus, discussions are necessary to address the contributions from those air plasmas. Actually, an experiment in Ref. 14 has already been carried out to ensure that THz waves generated with this focusing geometry are primarily from the plasmas located inside the water film. In this experiment, the focusing geometry is the same as that used in Ref. 14. The maximum excitation laser pulse energy 450  $\mu\text{J}$  is similar to that (400  $\mu\text{J}$ ) used in Ref. 14. Moreover, the larger angle of incidence onto the water film increases the laser path length within the water film, which also helps to hold the majority of the plasmas inside the water film.

To further compare the THz wave emission from the water film (at the focus) and that from the air plasma (at the interface) in the experiment, we can estimate the ratios of the corresponding THz electric field strength  $E_a(z_i)/E_w(z_0)$  and THz power  $P_a(z_i)/P_w(z_0)$ . The subscript  $w$  represents water and  $a$  represents air.  $z_0$  and  $z_i$  are the locations at the focus and the interface, respectively. It is assumed that no water is present when we estimate the values of  $E_a$  and  $P_a$ . The influence of the water film will be discussed later. We also assume that both the laser beam and the generated THz beam have a Gaussian profile for this approximation.

Under our experimental condition, the laser intensity in the air at the focus is assumed to be  $I(z_0) = 1 \times 10^{15} \text{ W/cm}^2$ .<sup>25,26</sup> The laser intensity  $I(z_i)$  at the interface is calculated through  $I(z_i) = I(z_0)[w(z_0)/w(z_i)]^2$ , where  $w(z_0)$  and  $w(z_i)$  are the radii of the laser beam at the focus and the interface, respectively. Thus, the ratio of generated THz electric field strength from the air at the focus to that at the interface  $E_a(z_i)/E_a(z_0)$  is calculated by the transient photocurrent model.<sup>7-9</sup> By experimentally measuring  $E_a(z_0)$  and  $E_w(z_0)$ , the ratio  $E_a(z_i)/E_w(z_0) = E_a(z_i)/E_a(z_0) \times E_a(z_0)/E_w(z_0) = 0.05\%$  is obtained. Then, the ratio of the THz intensity  $I_a(z_i)/I_w(z_0)$  is calculated from  $E_a(z_i)/E_w(z_0)$ . Finally, the ratio of the THz power  $P_a(z_i)/P_w(z_0) = 0.02\%$  can be obtained by integrating the corresponding THz intensity over its cross-section.

Consequently, the THz wave radiation from the air at the interface is negligible, in comparison to the contribution from the water film. In fact, the measurable THz field from the air plasmas at the interfaces should be even smaller. Specifically, the water film will either absorb 83% of the THz energy from the plasma located close to the first interface (air-water) or decrease the laser intensity by affecting the focusing geometry for the plasma near the second interface (water-air). Based on the above discussion, THz waves generated in the experiment are mainly attributed to the plasma within the water film rather than the air plasma.

In summary, the modulation of THz waves generated from liquid water with an asymmetric excitation scheme is achieved by adjusting the relative phase between  $\omega$  and  $2\omega$  pulses. The method also enables us to observe modulated and unmodulated THz waves with a Golay cell. By increasing the excitation laser pulse energy, the modulated component is quadratically enhanced above the threshold while the unmodulated component is linearly raised. Additionally, the generated THz energy is about two-orders of magnitude stronger than that with the one-color excitation scheme when short laser pulses are used. Besides providing an approach to reveal more information about plasma behaviors in liquids, this work offers an insight into developing a liquid THz source that may have applications in THz nonlinear optics and THz-driven electron acceleration.

The research at University of Rochester was sponsored by the Army Research Office under Grant No. W911NF-17-1-0428 and the Air Force Office of Scientific Research under Grant No. FA9550-18-1-0357; Jianming Dai at Tianjin University was supported by the National Natural Science Foundation of China under Grant No. 61875151 and the National Key Research and Development Program of China under Grant No. 2017YFA0701000.

- <sup>1</sup>D. J. Cook and R. M. Hochstrasser, *Opt. Lett.* **25**(16), 1210 (2000).
- <sup>2</sup>M. Kreß, T. Löffler, M. D. Thomson, R. Dörner, H. Gimpel, K. Zrost, T. Ergler, R. Moshhammer, U. Morgner, J. Ullrich, and H. G. Roskos, *Nat. Phys.* **2**, 327 (2006).
- <sup>3</sup>P. Gaal, W. Kuehn, K. Reimann, M. Woerner, T. Elsaesser, and R. Hey, *Nature* **450**, 1210–1213 (2007).
- <sup>4</sup>H. G. Roskos, M. D. Thomson, M. Kreß, and T. Löffler, *Laser Photonics Rev.* **1**(4), 349 (2007).
- <sup>5</sup>J. Dai, J. Liu, and X. C. Zhang, *IEEE J. Sel. Top. Quantum Electron.* **17**(1), 183 (2011).
- <sup>6</sup>X. Xie, J. Dai, and X. C. Zhang, *Phys. Rev. Lett.* **96**(7), 075005 (2006).
- <sup>7</sup>K. Y. Kim, J. H. Glowina, A. J. Taylor, and G. Rodriguez, *Opt. Express* **15**(8), 4577 (2007).
- <sup>8</sup>K.-Y. Kim, A. J. Taylor, J. H. Glowina, and G. Rodriguez, *Nat. Photonics* **2**(10), 605 (2008).
- <sup>9</sup>K.-Y. Kim, *Phys. Plasmas* **16**(5), 056706 (2009).
- <sup>10</sup>N. Karpowicz and X.-C. Zhang, *Phys. Rev. Lett.* **102**(9), 093001 (2009).
- <sup>11</sup>J. Dai, N. Karpowicz, and X.-C. Zhang, *Phys. Rev. Lett.* **103**(2), 023001 (2009).
- <sup>12</sup>H. Wen and A. M. Lindenberg, *Phys. Rev. Lett.* **103**(2), 023902 (2009).
- <sup>13</sup>J. Dai and X. C. Zhang, *Opt. Lett.* **39**(4), 777 (2014).
- <sup>14</sup>Q. Jin, Y. E. K. Williams, J. Dai, and X.-C. Zhang, *Appl. Phys. Lett.* **111**(7), 071103 (2017).
- <sup>15</sup>I. Dey, K. Jana, V. Y. Fedorov, A. D. Koulouklidis, A. Mondal, M. Shaikh, D. Sarkar, A. D. Lad, S. Tzortzakakis, and A. Couairon, *Nat. Commun.* **8**(1), 1184 (2017).
- <sup>16</sup>Y. Shen, T. Watanabe, D. A. Arena, C.-C. Kao, J. B. Murphy, T. Y. Tsang, X. J. Wang, and G. L. Carr, *Phys. Rev. Lett.* **99**(4), 043901 (2007).
- <sup>17</sup>D. Turchinovich, J. M. Hvam, and M. C. Hoffmann, *Phys. Rev. B* **85**(20), 201304 (2012).
- <sup>18</sup>E. A. Nanni, W. R. Huang, K.-H. Hong, K. Ravi, A. Fallahi, G. Moriena, R. J. Dwayne Miller, and F. X. Kärtner, *Nat. Commun.* **6**, 8486 (2015).
- <sup>19</sup>D. Zhang, A. Fallahi, M. Hemmer, X. Wu, M. Fakhari, Y. Hua, H. Cankaya, A.-L. Calendron, L. E. Zapata, and N. H. Matlis, *Nat. Photonics* **12**, 336–342 (2018).
- <sup>20</sup>Q. Wu and X.-C. Zhang, *Appl. Phys. Lett.* **67**(24), 3523 (1995).
- <sup>21</sup>P. K. Kennedy, *IEEE J. Quantum Electron.* **31**(12), 2241 (1995).
- <sup>22</sup>J. Noack and A. Vogel, *IEEE J. Quantum Electron.* **35**(8), 1156 (1999).
- <sup>23</sup>H. Hamster, A. Sullivan, S. Gordon, W. White, and R. W. Falcone, *Phys. Rev. Lett.* **71**(17), 2725 (1993).
- <sup>24</sup>P. K. Kennedy, D. X. Hammer, and B. A. Rockwell, *Prog. Quantum Electron.* **21**(3), 155 (1997).
- <sup>25</sup>P. Prem Kiran, S. Bagchi, S. R. Krishnan, C. L. Arnold, G. Ravindra Kumar, and A. Couairon, *Phys. Rev. A* **82**(1), 013805 (2010).
- <sup>26</sup>X.-L. Liu, X. Lu, X. Liu, T.-T. Xi, F. Liu, J.-L. Ma, and J. Zhang, *Opt. Express* **18**(25), 26007 (2010).